

Avalanchelike magnetic relaxation in the peak-effect regime of a Nb-O solid solution

Y. Kopelevich and S. Moehlecke

Instituto de Física "Gleb Wataghin," Universidade Estadual de Campinas, Unicamp 13083-970, Campinas, São Paulo, Brazil

(Received 28 October 1997; revised manuscript received 29 January 1998)

An increase of the pinning of vortices near the upper critical field boundary, the peak effect (PE), is studied in a Nb-O solid solution by means of the magnetization measurements. The PE onset is understood as a disorder-induced transition between a relatively ordered vortex lattice and an entangled vortex state. It is found that a characteristic feature of the vortex state in the PE region is a relaxation occurring via a large size magnetization jump or avalanche. It is also found that the temperature and field-dependent time $t_j(H, T)$, at which the jump occurs, quasi diverges at the peak field $H_p(T)$. [S0163-1829(98)04929-7]

The peak effect (PE), i.e., a maximum in the field and temperature dependence of the critical current density j_c , takes place in a vicinity of the upper critical field $H_{c2}(T)$ boundary, as in the case of low- T_c type-II superconductors (e.g., Refs. 1–3), or well below $H_{c2}(T)$, as in the case of high- T_c superconductors (e.g., Refs. 4–8). In many aspects, the interest in this effect is triggered by its possible relation to phase transition(s) of the flux-line lattice (FLL). Thus, experiments performed on $\text{YBa}_2\text{Cu}_3\text{O}_{7-\delta}$ provide evidence that the PE takes place just below the thermally-induced FLL melting phase transition,^{5,6} which was attributed to the softening of the FLL shear modulus c_{66} .⁹ The coexistence of solid and liquid vortex phases in the transition region has also been reported.^{10,11} Magnetotransport measurements performed on low- T_c superconductor 2H-NbSe_2 (Ref. 2) suggest the coincidence of the maximum in $j_c(T, H)$ with the melting transition of the vortex solid. The PE onset resulting from a disorder-induced transition between the FLL and an entangled vortex state has been discussed for both high- T_c (e.g., Refs. 12–14) and low- T_c (Ref. 3) superconductors. Besides, in the presence of a driving force, various dynamic transitions, i.e., transformations of the moving vortex states are also expected, where pinning plays a crucial role.^{2,15–20} All these bring the investigation of the vortex behavior in the PE region to the class of one of the most important problems of the mixed state of type-II superconductors.

In this work, the PE is studied in a Nb-O solid solution by means of magnetic measurements. It is found that a characteristic feature of the vortex state in the PE region is a relaxation occurring via a large size magnetization jump. It is also found that the time $t_j(H, T)$, at which the jump occurs, quasi diverges at the peak field $H_p(T)$.

The studied sample was prepared by heat treating an Nb single crystal ($T_c=9.2$ K), obtained from the Materials Research Corporation, at 1950 °C for 10 h in a vacuum pressure of 1×10^{-5} Torr followed by cooling to room temperature. No PE was observed in the virgin crystal. By comparing the obtained values of a zero-field $T_c=6.8$ K, lattice parameter expansion $\sim 0.36\%$, residual resistivity $\rho_r=10 \mu\Omega$ cm, and the residual resistivity ratio=2 with the literature data,²¹ we estimate an oxygen concentration of $\sim 2.5 \pm 0.5$ at. %, that is below the solubility limit of 3.5 at. %. Scanning electron microscopy analysis shows no segregation implying an uniform oxygen distribution.

The magnetization $M(H, T, t)$ measurements were made using a commercial superconducting quantum interference device magnetometer (Quantum Design-MPMS5) with field H applied along the longest size of the sample ($a \times b \times c = 2.8 \times 1.95 \times 0.7$ mm³). A careful investigation of the field inhomogeneity effect^{22,23} has been performed at all measured temperatures and fields, and no such effect was detected for scan lengths less than 2 cm. Thus, all measurements were performed with a scan length of 1.5 cm. Time relaxation measurements of M were made in both flux entrance and flux exit regimes. In the former case, the sample was cooled down to a target temperature in a zero applied magnetic field, and after temperature stabilization, the measuring field was applied. In the other case, the sample was cooled down in an applied field $H > H_{c2}(T)$, and then the field H was reduced to the measuring value.

Figure 1 shows the pinning force $F_p = j_c H$ vs H , obtained from $M(H)$ hysteresis loops measured at various temperatures, see inset. Figure 1 demonstrates clearly the occurrence of the PE in the sample studied here. The critical current density j_c was calculated according to the Bean's critical-state model using the formula $j_c(\text{A/cm}^2) = 30M_{hw}(G)/(c/2)$ (cm), where $M_{hw}(H) = (\frac{1}{2})[M^+(H) - M^-(H)]$ is the half width of the loop, and M^+ , M^- are the magnetizations

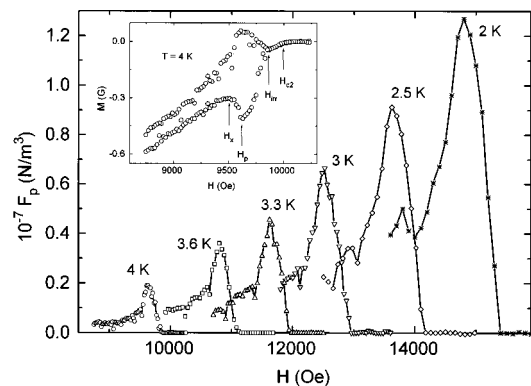


FIG. 1. The volume pinning force F_p vs field dependencies obtained from magnetization hysteresis loops $M(H)$ measured at various temperatures. Inset shows an example of the $M(H)$ dependence measured at $T=4$ K, where H_x is the PE onset field, H_p is the field corresponding to the maximum of F_p , H_{irr} is the irreversibility field, and H_{c2} is the upper critical field.

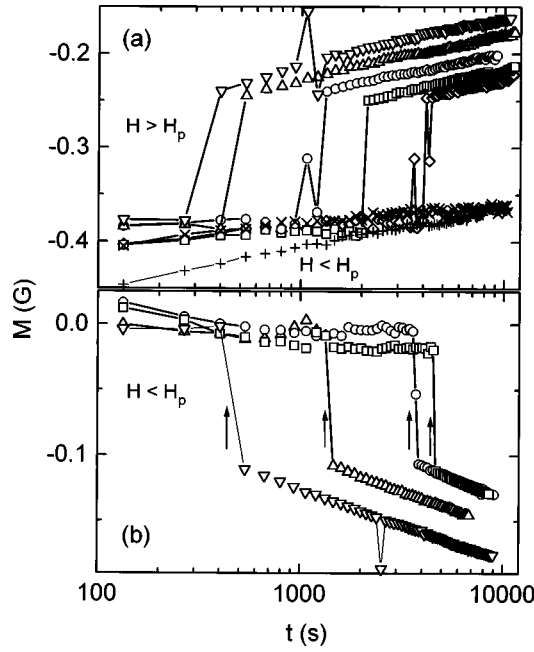


FIG. 2. Magnetic relaxation curves measured at $T=3.6$ K in the PE region ($H > H_x = 1.066$ T). (a) $M(t)$ dependencies measured in the flux entry regime both below and above the peak field $H_p = 1.08$ T: (\times) 1.07 T, ($+$) 1.074 T, (\diamond) 1.093 T, (\square) 1.0935 T, (\circ) 1.095 T, (Δ) 1.096 T, (∇) 1.097 T. (b) $M(t)$ dependencies measured in the flux exit regime at $H < H_p$: (∇) 1.068 T, (Δ) 1.07 T, (\circ) 1.072 T, (\square) 1.074 T. Arrows mark the jumping time $t_j(H)$.

corresponding to the ascending and descending branches of the hysteresis loop, respectively. The PE onset field H_x is determined by the point where a sharp increase of the $|M^+(H)|$ upon increasing field starts. The peak field H_p , corresponding to the maximum of F_p , the irreversibility field H_{irr} , and the upper critical field H_{c2} are also indicated in the inset of Fig. 1 [$H_x(T)$, $H_p(T)$, $H_{irr}(T)$, and $H_{c2}(T)$ are shown in the inset of Fig. 5]. The height of the $F_p(H)$ peak gradually decreases with temperature (see Fig. 1), and at $T > 4.5$ K ($t = T/T_c > 0.66$) becomes smaller than our resolution limit.

Figures 2(a) and 2(b) show magnetization relaxation curves $M(t)$ measured at $T=3.6$ K and at various applied fields $H > H_x = 1.066$ T, i.e., in the PE region, in both flux entry (a) and flux exit (b) regimes. As can be seen in Fig. 2(a), a characteristic feature of the $M^+(t)$ relaxation curves in the flux entry regime and at $H > H_p = 1.08$ T is the sudden jump of $|M^+|$ towards a smaller value at a field-dependent ‘‘jumping’’ time $t_j(H, T)$, whereas at $H < H_p$ the relaxation is smooth. In contrast, in the flux exit regime the jumplike reduction of $|M^-|$ at the time $t_j(H, T)$ takes place only at $H < H_p$ [see Fig. 2(b); here the relaxation curves at $H > H_p$ are not shown for clarity]. A similar behavior was found at all temperatures $T \leq 3.6$ K. At higher temperatures, however, the avalanches occur both below and above $H_p(T)$, and in both relaxation regimes. Figure 3 illustrates this fact, showing the jumping time $t_j(H, T)$ vs $H/H_p - 1$ measured at $T = 2, 3.6,$ and 4 K. This figure clearly demonstrates the steep increase of $t_j(H, T)$ as the measuring field tends to $H_p(T)$. We emphasize that the observed $t_j(H, T)$ is very well reproducible as confirmed by numerous measurements. Another

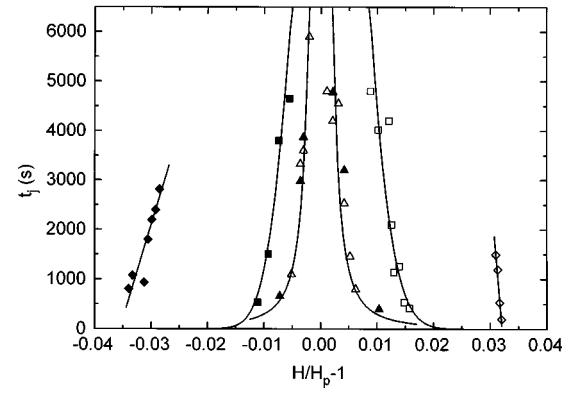


FIG. 3. The jumping time $t_j(H, T)$ vs $(H/H_p - 1)$ measured at $T=2$ K (diamonds), $T=3.6$ K (squares), and $T=4$ K (triangles). Open symbols correspond to the data obtained in the vortex entry regime, whereas solid symbols correspond to the data obtained in the vortex exit regime. Solid lines are a guide for the eye.

characteristic feature of the $M(t)$ dependencies is an essential slowing down of the relaxation ($dM/dt \rightarrow 0$) as t tends to $t_j(H, T)$ (see Fig. 2). Note also that no jump in $M(t)$ was detected in the field interval $H_{c1}(T) < H < H_x(T)$, i.e., outside of the PE region. This is shown in Fig. 4 where $M(t)$ measured at $T=3$ K and $H < H_x = 1.235$ T in both vortex entry and vortex exit regimes is presented. For completeness, $M^+(t)$, obtained for various fields above the peak field $H_p = 1.25$ T, i.e., in the jumpy region, is also shown in the inset of Fig. 4.

Magnetic relaxation in type-II superconductors, in general, results from the vortex motion driven by the gradient of the vortex density. When the pinning is sufficiently weak, the moving object is a relatively ordered FLL. However, in the strong pinning limit, when disorder dominates over intervortex interaction, the FLL breaks up and the plastic motion of some regions of the FLL with respect to other temporarily pinned regions takes place. This plastic motion, occurring via intermittent avalanches, was directly observed in Nb films at low fields and temperatures by means of the Lorentz microscopy.²⁴

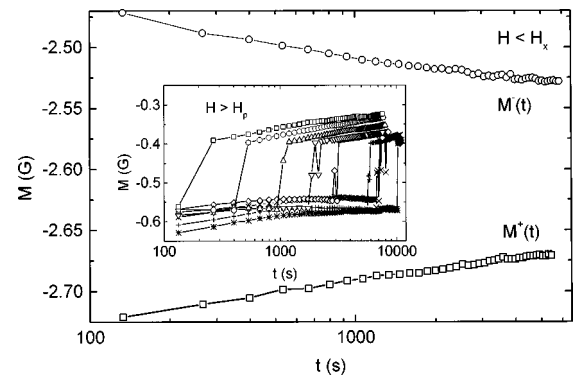


FIG. 4. Magnetic relaxation curves $M(t)$ measured at $T=3$ K and $H=0.8$ T, below the PE onset field $H_x = 1.235$ T, M^+ and M^- are magnetizations corresponding to the ascending and descending branches of the hysteresis loop $M(H)$, respectively. Inset shows $M(t)$ dependencies measured in the flux entry regime above the peak field $H_p = 1.25$ T: (\square) 1.264 T, (\circ) 1.263 T, (Δ) 1.262 T, (∇) 1.261 T, (\diamond) 1.2605 T, ($+$) 1.26 T, (\times) 1.2595 T, ($*$) 1.259 T.

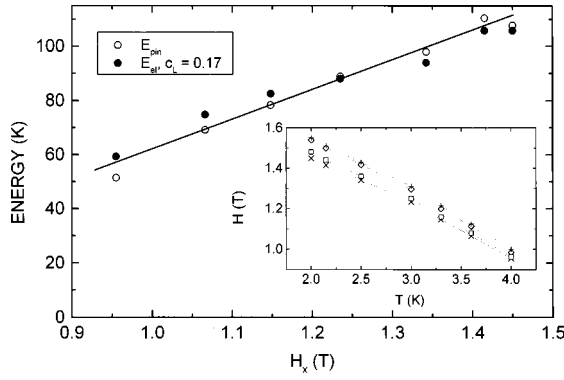


FIG. 5. The pinning E_{pin} and elastic E_{el} energies calculated along the $H_x(T)$ boundary. Solid line is a guide for the eye. Inset: (\times) $H_x(T)$, (\square) $H_p(T)$, (\diamond) $H_{\text{in}}(T)$, and ($+$) $H_{c2}(T)$.

In the present work, we believe that a similar phenomenon is found in the PE region. However, our observation of a single avalanchelike event during hours of relaxation (here we do not consider the rare occasionally happened ‘‘reversible’’ magnetization jumps) differs from Ref. 24, where time intervals between avalanches are found to be of the order of a few seconds. This fact, as well as the absence of a jump in $M(t)$ in the field range $H_{c1}(T) < H < H_x(T)$, implies that the magnetization jump observed at $t_j(H, T)$ is a characteristic feature of the vortex dynamics in the PE region. It should be noted that the plastic vortex motion occurring just above the PE onset field $H_x(T)$ was also found in Ref. 2.

Recently, it has been suggested that the onset of the PE is associated with the formation of an entangled vortex state, where vortex dynamics governed by plastic deformations is expected.^{12–14} According to the theory, this disorder-driven transition (or crossover) between the FLL and the entangled vortex state results from the competition between vortex-vortex interaction and the strength of the quenched disorder (pinning), and is determined by the balance between the elastic $E_{\text{el}} = c_L^2 a_0^2 (c_{66} \epsilon_0)^{1/2}$ and pinning $E_{\text{pin}} = (WL_0 \xi^4)^{1/2}$ energies, as obtained within a cage model using the Lindemann criterion.^{12–14} Here $c_L \sim 0.1–0.3$ is the Lindemann number, $a_0 = (2\pi)^{1/2} \xi$ is the intervortex spacing near $H_{c2}(T)$, $c_{66} = [(1 - 1/2\kappa^2)/8\mu_0\kappa^2] H_{c2}^2 b(1-b)^2(1-0.29b)$,²⁵ $\epsilon_0 = (\Phi_0^2/4\pi\mu_0\lambda^2) \ln \kappa$ is the vortex line energy, and $L_0 = (\epsilon_0/c_{66})^{1/2}$ is the longitudinal size of the elastic cage, which in our case is less than the three-dimensional longitudinal collective pinning length $L_c = (c_{44}/c_{66})^{1/2} R_c$,²⁶ $c_{44} = (H^2/\mu_0\kappa^2)(1-b)$ is the FLL tilt modulus, and $R_c = 8\pi r_p^2 c_{44}^{1/2} c_{66}^{3/2}/W$ is the transverse correlation radius with the range of the pinning force $r_p \approx \xi$. The parameter W , which measures the pinning strength, is $W = (F_p r_p^3 c_{66}^2 c_{44})^{1/2} / (1.5^{1/2}/32\pi^2)^{1/2}$.²⁵ Results of the calculation of both E_{el} and E_{pin} , taking the sample parameters determined in this work $\kappa = 7.8$, $\xi(0) = 135 \text{ \AA}$ and the measured volume pinning force F_p (Fig. 1), are presented in Fig. 5. As seen, the elastic energy E_{el} perfectly matches the pinning energy E_{pin} at $H = H_x(T)$, using the Lindemann number $c_L = 0.17$ as a free parameter, which suggests the occurrence of the entangled vortex state at $H \geq H_x(T)$ in our sample.

A plastic vortex motion in the entangled state can take place by reptation or via cutting and reconnection of the

vortex lines.^{12,27,28} The here observed steep rise of the jumping time $t_j(H, T)$ when H tends to the peak field $H_p(T)$, see Fig. 3, i.e., as the critical current tends to its maximal value, also gives evidence that the effective strength of the pinning plays a crucial role in the occurrence of the avalanches. Next, we speculate on a possible origin of the $t_j(H, T)$.

We assume that in the field interval $H_x(T) < H < H_p(T)$, the jump in $M(t)$ is related to a vortex disentanglement process occurring by reptation, whereas above $H_p(T)$, the dominant process is due to vortex cutting and reconnection. According to the reptation models^{27,28} the relaxation time [$\tau \sim t_j(H, T)$] is a steep increasing function of the wandering distance u_0 , induced either by thermal fluctuations or quenched disorder. The increase of the pinning efficiency of vortices with field implies an increase of the disorder-induced wandering distance u_0 , and therefore $t_j(H, T)$. On the other hand, as H tends to $H_p(T)$, the density of dislocations increases and the vortex cutting becomes easier,¹² so at $H > H_p(T)$ the disentanglement, occurring via vortex cutting and reconnection is the dominant process. In this case, the relaxation time $\tau \sim t_j(H, T) \sim \exp(U_x/k_B T)$,^{12,29–31} where U_x is the crossing energy, which decreases with field. Accordingly, in the field interval $H_p(T) < H < H_{c2}(T)$, the $t_j(H, T)$ decreases with field. Thus, this qualitative picture can describe the $t_j(H, T)$ in both vortex entry and vortex exit regimes below and above the peak field $H_p(T)$, at least at $T = 4 \text{ K}$ (see Fig. 3). Note also that as H tends to the $H_x(T)$ from above, a sequential disentanglement process, described in Ref. 28, instead of the reptation mechanism, can dominate; in both cases $t_j(H, T)$ should decrease as H approaches $H_x(T)$.

At low temperatures ($< 4 \text{ K}$), the magnetization jump in $M(t)$ was observed only for $H > H_p(T)$ under increasing field and for $H < H_p(T)$ under decreasing field (see Figs. 2 and 3). This behavior, different from that found at $T = 4 \text{ K}$, could be due to an increasing role of the quenched disorder at lower temperatures (a different behavior for leaving and entering vortices caused by disorder has already been reported for other superconductors^{32,33}). Consider first the ascending branch of the $M(H)$. For the same reduced field $h = H/H_{c2}(T)$, the low-temperature disorder-induced wandering distance u_0 is larger, as compared to that at high temperatures, due to the increase of the pinning efficiency of the vortices (see Fig. 1). According to reptation models,^{27,28} this leads to an increase of the relaxation time. Thus, at low temperatures the $t_j(H, T)$ in the flux entry regime and for $H_x(T) < H < H_p(T)$ can become longer than the experimental observation time t_{obs} . Above the peak field $H_p(T)$, the crossing energy U_x is small enough at all temperatures in the vortex entry regime, allowing us to observe the magnetization jump within the explored time window. On the other hand, crossing barriers for the vortex exit [$H_p(T) < H < H_{c2}(T)$] can be larger than the barriers for the vortex entry, assuming lower density of disorder-induced dislocations for the vortex exit branch of the hysteresis loop. Thus, under decreasing field and for $H_p(T) < H < H_{c2}(T)$, the relaxation time [$\tau \sim t_j(H, T) \sim \exp(U_x/k_B T)$] can exceed that in the field increasing regime, i.e., $t_j(H, T) > t_{\text{obs}}$. As the field further decreases [tends to the $H_x(T)$], the sequential disentanglement

ment process, faster than the disentanglement by reptation,²⁸ can be responsible for the observed $t_j(H, T)$.

Thus, the above given scenario suggests that for $H > H_p(T)$ the vortex cutting is the dominant relaxation process, i.e., the irreversible magnetization $M_{\text{irr}}(H) \sim M_{\text{hw}}(H)$ is mostly due to the vortex ability to sustain a current (associated with a gradient in the vortex density) without flux-line cutting occurring. Accordingly, the loss of the $M_{\text{irr}}(H)$ at $H \geq H_p(T)$ (see the insets in Figs. 1 and 4) can be related to a thermally activated vortex cutting process as the relaxation time $\sim \exp(U_x/k_B T)$ becomes comparable to the measuring time.

Finally, noting that the quasi divergence of $t_j(H, T)$ at $H = H_p(T)$ (Fig. 3) resembles very much an approach to a phase transition that might be related to the onset of the

vortex cutting and reconnection process. Whether a true phase transition takes place at the peak field $H_p(T)$ remains an interesting problem for further studies.

To conclude, we have studied the peak effect in a Nb-O solid solution single crystal. This effect is understood as a disorder-driven transition (or crossover) between a relatively ordered vortex lattice and an entangled vortex state. We found that the characteristic relaxation process in the peak-effect region is a magnetization jump occurring at a time $t_j(H, T)$ that quasi diverges at the peak field $H_p(T)$.

The authors are grateful to P. Esquinazi for a critical reading of the manuscript and A. E. Koshelev for comments. This work was partially supported by FAPESP Proc. No. 95/4721-4 and CNPq Proc. Nos. 300862/85-7 and 301216/93-2.

- ¹R. Wördenweber, P. H. Kes, and C. C. Tsuei, *Phys. Rev. B* **33**, 3172 (1986); R. Wördenweber and P. H. Kes, *ibid.* **34**, 494 (1986).
- ²S. Bhattacharya and M. J. Higgins, *Phys. Rev. Lett.* **70**, 2617 (1993); M. J. Higgins and S. Bhattacharya, *Physica C* **257**, 232 (1996).
- ³P. L. Gammel, U. Yaron, A. P. Ramirez, D. J. Bishop, A. M. Chang, R. Ruel, L. N. Pfeiffer, E. Bucher, G. D'Anna, D. A. Huse, K. Mortensen, M. R. Eskildsen, and P. H. Kes, *Phys. Rev. Lett.* **80**, 833 (1998).
- ⁴X. S. Ling and J. I. Budnick, in *Magnetic Susceptibility of Superconductors and Other Spin Systems*, edited by R. A. Hein, T. L. Francavilla, and D. H. Liebenberg (Plenum, New York, 1991), p. 377.
- ⁵W. K. Kwok, J. A. Fendrich, C. J. van der Beek, and G. W. Crabtree, *Phys. Rev. Lett.* **73**, 2614 (1994).
- ⁶J. Giapintzakis, R. L. Neiman, D. M. Ginsberg, and M. A. Kirk, *Phys. Rev. B* **50**, 16 001 (1994).
- ⁷M. Ziese, P. Esquinazi, A. Gupta, and H. F. Braun, *Phys. Rev. B* **50**, 9491 (1994).
- ⁸B. Khaykovich, E. Zeldov, D. Majer, T. W. Li, P. H. Kes, and M. Konczykowski, *Phys. Rev. Lett.* **76**, 2555 (1996).
- ⁹A. I. Larkin, M. C. Marchetti, and V. M. Vinokur, *Phys. Rev. Lett.* **75**, 2992 (1995).
- ¹⁰J. A. Fendrich, U. Welp, W. K. Kwok, A. E. Koshelev, G. W. Crabtree, and B. W. Veal, *Phys. Rev. Lett.* **77**, 2073 (1996).
- ¹¹S. N. Gordeev, A. P. Rassau, D. Bracanovic, P. A. J. de Groot, R. Gagnon, and L. Taillefer, *Applied Superconductivity 1997*, **1**, 1113–1116, IOP Conf. Proc. No. 158 (Institute of Physics and Physical Society, London, 1997).
- ¹²D. Ertas and D. R. Nelson, *Physica C* **272**, 79 (1996).
- ¹³D. Giller, A. Shaulov, R. Prozorov, Y. Abulafia, Y. Wolfus, L. Burlachkov, Y. Yeshurun, E. Zeldov, V. M. Vinokur, J. L. Peng, and R. L. Greene, *Phys. Rev. Lett.* **79**, 2542 (1997).
- ¹⁴V. Vinokur, B. Khaykovich, E. Zeldov, M. Konczykowski, R. A. Doyle, and P. H. Kes, *Physica C* **295**, 209 (1998).
- ¹⁵H. J. Jensen, A. Brass, and A. J. Berlinsky, *Phys. Rev. Lett.* **60**, 1676 (1988).
- ¹⁶A.-C. Shi and A. J. Berlinsky, *Phys. Rev. Lett.* **67**, 1926 (1991).
- ¹⁷A. E. Koshelev and V. M. Vinokur, *Phys. Rev. Lett.* **73**, 3580 (1994).
- ¹⁸S. Ryu, M. Hellerqvist, S. Doniach, A. Kapitulnik, and D. Stroud, *Phys. Rev. Lett.* **77**, 5114 (1996).
- ¹⁹M. C. Faleski, M. C. Marchetti, and A. A. Middleton, *Phys. Rev. B* **54**, 12 427 (1996).
- ²⁰S. Spencer and H. J. Jensen, *Phys. Rev. B* **55**, 8473 (1997).
- ²¹C. C. Koch, J. O. Scarbrough, and D. M. Kroeger, *Phys. Rev. B* **9**, 888 (1974).
- ²²A. D. Huxley, C. Paulsen, O. Laborde, J. L. Tholence, D. Sanchez, A. Junod, and R. Calemczuk, *J. Phys.: Condens. Matter* **5**, 7709 (1993).
- ²³G. Ravikumar, T. V. Chandrasekhar Rao, P. K. Mishra, V. C. Sahni, S. Saha, S. S. Banerjee, N. G. Patil, A. K. Grover, S. Ramakrishnan, S. Bhattacharya, E. Yamamoto, Y. Haga, M. Hedo, Y. Inada, and Y. Onuki, *Physica C* **276**, 9 (1997).
- ²⁴T. Matsuda, K. Harada, H. Kasai, O. Kamimura, and A. Tonomura, *Science* **271**, 1393 (1996).
- ²⁵E. H. Brandt, *Int. J. Mod. Phys. B* **5**, 751 (1991); *Rep. Prog. Phys.* **58**, 1465 (1995).
- ²⁶A. I. Larkin and Yu. N. Ovchinnikov, *J. Low Temp. Phys.* **34**, 409 (1979).
- ²⁷D. R. Nelson and H. S. Seung, *Phys. Rev. B* **39**, 9153 (1989).
- ²⁸S. P. Obukhov and M. Rubinstein, *Phys. Rev. Lett.* **65**, 1279 (1990).
- ²⁹D. R. Nelson and M. C. Marchetti, *Phys. Rev. B* **42**, 9938 (1990).
- ³⁰M. E. Cates, *Phys. Rev. B* **45**, 12 415 (1992).
- ³¹C. Carraro and D. S. Fisher, *Phys. Rev. B* **51**, 534 (1995).
- ³²S. Senoussi, A. Kilic, P. Manuel, R. Gagnon, L. Taillefer, and H. Traxler, *Physica C* **264**, 172 (1996).
- ³³Y. Kopelevich, V. V. Makarov, and S. Moehlecke, *Physica C* **277**, 225 (1997).